

EFFECT OF CHARGE DEPTH IN RUSSIAN HYDROACOUSTIC DATA FROM NUCLEAR AND HE EXPLOSIONS

Mariana Eneva, Jeffrey L. Stevens, and Jack Murphy
Maxwell Technologies/Systems Division

Boris D. Khristoforov
Institute for Dynamics of the Geospheres, Russian Academy of Sciences

Sponsored by the Defense Threat Reduction Agency
Contract No. DSWA01-97-C-0166

ABSTRACT

In a collaborative effort to understand better the coupling of energy from explosions near the water surface, we examine and analyze unique hydroacoustic data from the Russian archives. This is important to CTBT monitoring, because the hydroacoustic energy from such blasts is greatly diminished by comparison with deeply immersed charges. The data include peak pressure measurements and hydrophone records from nuclear explosions, as well as a comprehensive digitized data set from 100-kg TNT explosions in a reservoir. Our work includes the continued use of the REFMS code for modeling of shock-wave reflection and refraction in multi-layered ocean and ocean bottoms. We also study relevant Russian publications reporting on the HE experiments and make comparisons with existing relationships depicting the dependence of the coupling coefficient on charge depth/height.

A number of near-surface nuclear blasts were carried out in the shallow waters (≤ 60 m) of the Bay of Chernaya (Novaya Zemlya) in the late 50's and early 60's. Data is available from three of these explosions. The first underwater nuclear blast (October 10, 1957) was reported with yield of 10 kt and charge depth of 30 m. Seven peak-pressure measurements are available from this explosion, which average about 300 kg/cm² at a 235-m distance and sensor depths 10 to 50 m. Hydrophone records from the two other nuclear blasts (October 23 and 27, 1961) are available at much larger distances, 35 km to 160 km, at sensor depths of 1 m above the bottom. These records show levels of sound pressure measured in three different bands from low to high frequencies. The records from the first of these nuclear explosions, of yield 4.8 kt and charge depth 20 m, indicate peak levels of sound pressure between 103 dB and 125 dB. The records from the second 1961 nuclear explosion, of 16-kt yield and height above water 1.1 m, show levels between 90 dB and 130 dB, with the pressure of the direct shock wave being diminished to ~4% of the pressure that would have been observed in boundless water. Distinct arrivals are seen for both 1961 blasts, such as direct shock waves in water (T-phase), refractions in the crust and the bottom layers, and signals corresponding to sound speed of shock waves in air.

Continuing our earlier analysis of pressure-time histories from the 100-kg TNT experiments in a reservoir, we are using the latest REFMS version to model the digitized hydroacoustic measurements from twelve explosions with charge depths from 0 to 2.75 m. In addition to pressure data, the complete data set now includes impulse and energy data as well. The modeling results match the peak-pressure observations rather well, especially in mid-pool, where the measurements suggest free-water-like environment. The estimated pressure coupling coefficients for the shallowest charges, in the range of 30 to 70%, are compared with existing relationships. We find that while these relationships predict coupling to be independent of distance to sensor, our estimates based on the Russian HE data decrease with distance. This suggests that the coupling is more complex than in theory and may have to be adjusted for more accurate modeling of the effect of charge depth.

OBJECTIVE

The objective of this work is to analyze and model unique historical Russian data including hydroacoustic measurements from nuclear explosions in Novaya Zemlya and 100-kg TNT experiments in a reservoir of

water. The purpose is to evaluate decoupling of energy as a function of explosion depth, thus contributing to CTBT verification.

RESEARCH ACCOMPLISHED

Introduction

Understanding the difference in coupling from deep underwater explosions versus shallow and near surface explosions is of significant interest to CTBT verification. The reason is that while even small deep explosions generate signals easily observable at great distances in the world sound channel, shallow and surface explosions produce signals of significantly diminished energy. Therefore finding, analyzing and modeling hydroacoustic data featuring various combinations of explosion depths and distances to sensors, can be very useful in evaluating and modeling the difference in the effects of fully-immersed and shallow charges.

Unique historical Russian hydroacoustic data has become recently available from 100-kg TNT explosions conducted at various depths in a reservoir (Kozachenko and Khristoforov, 1970; Korobeinikov and Khristoforov, 1976) and from underwater and above-water nuclear explosions in the shallow Bay of Chernaya, Novaya Zemlya, detonated in 1957 and 1961 (*USSR Nuclear Weapons Tests and Peaceful Nuclear Explosions 1949 through 1990*, 1996). Eneva et al. (1999) have analyzed earlier pressure records from the 100-kg TNT data showing up to 60-70% decrease in peak pressure between half-immersed (0-m depth) and fully immersed charges, as well as several peak-pressure measurements from the 1957 underwater nuclear explosion. These data were modeled using a numerical code from the Computational Aids provided by DSWA (Stephens and Kelley, 1996). It was derived from a more comprehensive code for modeling of surface reflections, and bottom reflections and refractions due to sound-velocity gradients, known as REFMS. Details on the code can be found in Britt (1986) and more recent *REFMS User's Guides*. It is also discussed at some length in *Handbook of Nuclear Weapon Effects* (1996) – further referred to as *EM-1*. REFMS uses spherical wavefronts and finite-element calculations taking into account deviations from acoustic properties, i.e., nonlinear effects. It has been extensively validated and found in many cases to predict the underwater shock-wave environment with accuracy better than or comparable with hydrodynamic computations. This is significant, because the latter require much greater computer and labor resources. Still, REFMS is valid in relatively weakly nonlinear regimes and cannot replace hydrocodes in highly nonlinear environments. In our earlier work (Eneva et al., 1999), many of the measurements in the Russian experiments were predicted very well with REFMS, thus providing further validation of the code. These data and predictions were also compared with results from LLNL hydrodynamic calculations (Clarke et al., 1995). It was found that rates of change in peak pressures as charge depth increases in the Russian data are very similar to that predicted by REFMS, and somewhat similar to the LLNL predictions. However, the LLNL calculations for nuclear explosions were found to be much more similar to the high-explosive (HE) predictions of REFMS than to the nuclear REFMS calculations. The latter reach full coupling for much shallower explosion depths than in the hydrodynamic modeling; see Figures 6 and 7 in Eneva et al. (1999). In any case, these different approaches to modeling are not directly comparable and the relevance of small-scale HE tests to the study of the effect of charge depth of nuclear underwater explosions is not well understood.

Here we present results from the continuation of the above studies. We can now add archival records from one more underwater explosion and one above-water nuclear blast. Also, we now have the complete digitized data set from the twenty-nine 100-kg TNT experiments, including time histories of pressure and impulse (222 hydroacoustic records each, 36 records in air, and 50 in ground), and shock-wave parameters (peak pressures, specific impulse, pulse duration, and energy estimates). We have analyzed and modeled the hydroacoustic data from twelve experiments performed in a full reservoir (3-m water level). These are more relevant analogues for our purpose, as we seek to evaluate the effect of shallow explosions in relatively deep water, from which signals are likely to propagate to large distances in the SOFAR channel. In contrast, signals from explosions in shallow water are greatly diminished and are unlikely to reach the sound channel at above-noise level. Thus the remaining seventeen 100-kg TNT tests, carried out in very

shallow water (1-m and 0.5-m water level), are not considered at this time. We continue to apply REFMS modeling to the observations where possible, using its latest, 1999 version.

Nuclear Explosions in the Bay of Chernaya, Novaya Zemlya

Several underwater and above-water nuclear explosions of torpedoes have been carried out in the Bay of Chernaya during the period September 1955 - August 1962. Data are currently available for two of the underwater and one of the above-water explosions. Their location is shown on the map of the Bay of Chernaya in Figure 1. The torpedoes were launched from submarines in the vicinity of the strait connecting the bay with Barents Sea. In all three cases the geographic co-ordinates noted in the archival materials were the same - 70.70°N and 54.67°E. However, their locations must have not been exactly identical, as the reported depths of the bottom under the blasts differ. More details about these nuclear blasts are shown in Table 1 (*USSR Nuclear Weapons Tests and Peaceful Nuclear Explosions 1949 through 1990*, 1996). Yield values in parentheses represent different estimates in the literature.

Table 1. Archival data from three nuclear explosions in 1957 and 1961.

Date & Moscow time	Yield [kt]	Depth/Height Expl. [m]	Depth Bottom Under Expl. [m]	Distance to Sensors [km]	Depth Bottom Under Sensors [m]	Depth Sensors [m]	Available Data/ <u>Type of Sensor</u>
10/10/57 09:54:32	10	30 under	≤ 60	0.235	≤ 60	10-50	peak-pressure measurements/MID-3
10/23/61 13:30:47	4.8 (4)	20 under	47	34.84	50	49	sound, infra/hydrophones
				104.9	60	59	sound/hydrophones
10/27/61 11:30:26.6	16 (17.5)	1.1 above	59	34.84	50	49	sound, infra, ultra/ hydrophones
				160.5	45	44	infra/hydrophone

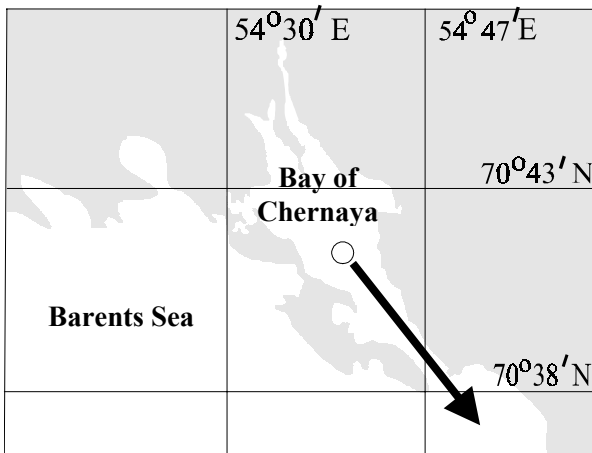
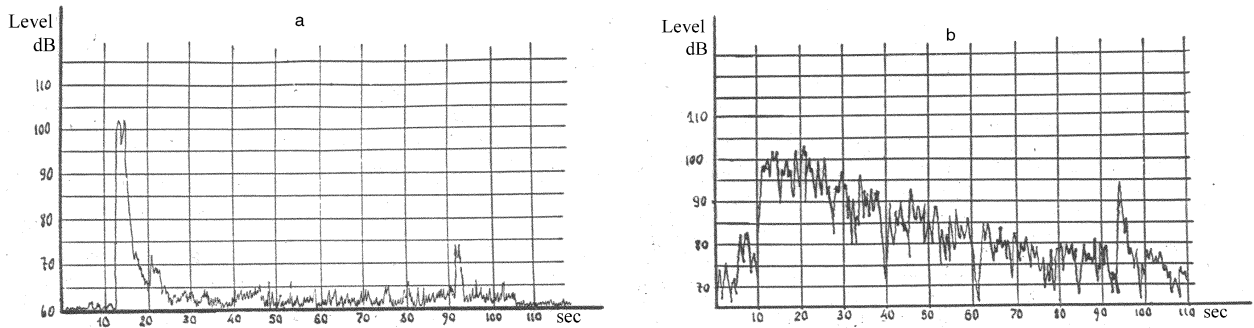


Figure 1. Map of the Bay of Chernaya (Novaya Zemlya). Circle shows location of two underwater and one above-water explosions (1957-1961). Arrow indicates direction to sensor locations, where long-

The measurements from the 1957 explosion were in the near field, while the hydroacoustic signals from the 1961 blasts were recorded at much larger distances. The exact geographic co-ordinates of the sensor locations are not available, but it is known for the 1961 explosions that measurements were taken along a line originating at the blast location and passing through the narrow strait connecting the bay with Barents Sea. The hydrophones were suspended at 1 m above the bottom in the case of the 1961 blasts and at various depths in the case of the 1957 explosion. The Russian archives cite sound velocity of 1430 m/s, characteristic for low-salinity water.

The peak-pressure measurements in the near field (235 m) from the 1957 underwater explosion were made at seven depths, using four to six sensors at each depth. Based on the average of these measurements (~300 kg/cm²) as compared with REFMS-predicted values and data from the 100-kg TNT experiments, Eneva et al. (1999)

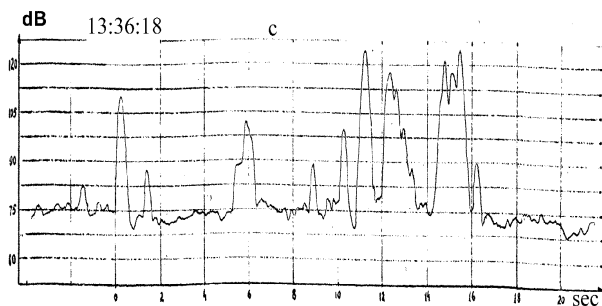
suggested that the explosion yield was probably not larger than 5 to 6 kt, versus the reported 10 kt (*USSR Nuclear Weapons Tests and Peaceful Nuclear Explosions 1949 through 1990*, 1996). More details can be



found in our earlier publication.

The hydroacoustic signals from the 1961 explosions were recorded with hydrophones suspended from ships at different distances (see Table 1), much further than the sensors used for the 1957 underwater explosion. Three channels with different filters were used, referred to as “sound”, “infrasound”, and “ultrasound” in the Russian archives. They correspond to frequency bands 60-10,000 Hz, 5-100 Hz, and 8-100 kHz, respectively. The records in Figures 2 to 5 are of somewhat compromised quality, as they were scanned from the archival materials. The level of sound pressure in these figures is shown in dB (decibels), better suited to represent small pressures. As a reminder, the pressure level p in the units of dB is given by $20 \times \log_{10}(p/p_0)$, where $p_0 = 2 \times 10^{-4} \text{ dyn/cm}^2 = 2 \times 10^{-5} \text{ Pa} = 2 \times 10^{-10} \text{ kg/cm}^2 = 0 \text{ dB}$, is the threshold of audibility. Thus, $1 \mu\text{bar} = 1 \text{ dyn/cm}^2 = 0.1 \text{ Pa} = 74 \text{ dB}$, $1 \text{ mbar} = 134 \text{ dB}$, and $100 \text{ mbar} = 174 \text{ dB}$ (e.g., a normal conversation is about 60 dB). An equivalent illustration of the dB-unit is in terms of intensity level (or energy), $10 \times \log_{10}(E/E_0)$, where the hearing threshold is $E_0 = 10^{-12} \text{ watts/m}^2$.

Figures 2 and 3 show records from the underwater 1961 explosion at two distances and in different frequency bands. In Fig. 2a (35-km distance), the time of explosion is placed at 0 s. The pre-signal noise levels are ~60 dB in the sound band of frequencies and ~70-80 dB in the infrasound band. The maximum signal levels in both cases reach 102-103 dB. As could be expected, attenuation is much less in the lower frequencies (Fig. 2b). Three distinct arrivals are observed in the sound band (Fig. 2a) – at ~12 s, ~21 s, and ~92 s. The corresponding effective sound velocities are ~2900 m/s, ~1660 m/s, and ~380 m/s, respectively. Thus the first arrival likely represents a wave reflected from the top of the crust and passing through the layer of deposits on the bottom. The low-



velocity third arrival may indicate propagation of shock wave in air, which can travel at larger velocities than that of regular acoustic waves. For such an arrival to be observed, the shock wave in air from the explosion plume must have propagated through an air sound channel and then refracted towards the water. As to the second arrival, it is a few seconds earlier than a direct shock hydroacoustic wave (T-phase) at 1430 m/s would arrive (i.e., at ~24.4 s). While such a phase is not seen in the higher-frequency band (Fig. 2a), the lower-frequency record (Fig. 2b) indicates substantial energy around 24.4 s, in a pack with earlier and later arrivals. Compared with the higher-frequency record (Fig. 2a), the onset of the first arrival is earlier in the low-frequency band (~10 s, or a velocity of ~3500 m/s), while the third arrival is later (~93-94s, or velocity of ~370-375 m/s).

velocity third arrival may indicate propagation of shock wave in air, which can travel at larger velocities than that of regular acoustic waves. For such an arrival to be observed, the shock wave in air from the explosion plume must have propagated through an air sound channel and then refracted towards the water. As to the second arrival, it is a few seconds earlier than a direct shock hydroacoustic wave (T-phase) at 1430 m/s would arrive (i.e., at ~24.4 s). While such a phase is not seen in the higher-frequency band (Fig. 2a), the lower-frequency record (Fig. 2b) indicates substantial energy around 24.4 s, in a pack with earlier and later arrivals. Compared with the higher-frequency record (Fig. 2a), the onset of the first arrival is earlier in the low-frequency band (~10 s, or a velocity of ~3500 m/s), while the third arrival is later (~93-94s, or velocity of ~370-375 m/s).

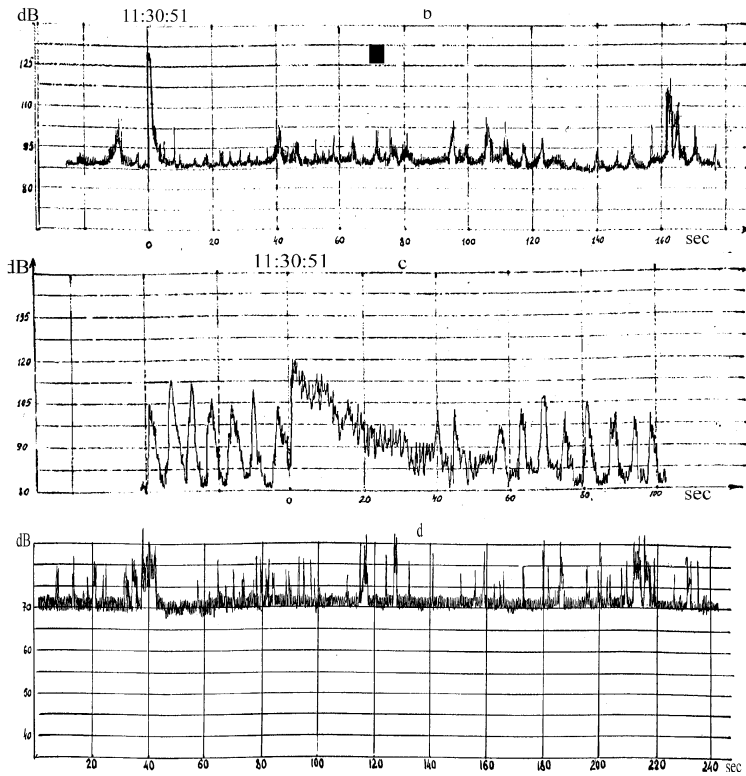


Figure 3 shows the available short portion (~25 s) of the record made in the sound band of frequencies, at a distance of ~105 km from the underwater 1961 explosion. The noise level is at ~75 dB, while the signal level reaches ~125 dB. The horizontal axis has its 0 at 13:36:18 Moscow time; i.e., 331 s after the time of explosion. Thus the earliest arrival observed on this record may have propagated mostly in air with a velocity of ~317 m/s. More energy is observed later, arriving at velocities ~310 m/s.

Figures 4 and 5 show records from the above-water 1961 nuclear explosion of 16-kt yield at two distances. The records in Fig. 4 have been made in the same location as the records from the underwater explosion, at a distance of ~35 km. The pre-signal noise levels were higher than four days earlier prior to the underwater explosion - ~90 dB, ~110 dB, and ~73 dB in the

sound, infrasound, and ultrasound bands, respectively. Maximum signal levels in the three bands were ~130 dB, ~120 dB, and ~90 dB. The sound records have their 0's on the time axes at 11:30:51 Moscow time, which is 24.4 s after the time of explosion (see Table 1). The direct shock wave (T-phase) is clearly seen, with corresponding significantly stronger attenuation for the higher frequencies (Fig. 4a). A smaller arrival ~12 s earlier in the sound record, is likely to be of the same type as the first arrival in the records from the underwater explosion, i.e., reflected in the crust and passing through the sediments on the bottom. It is not seen, however, in the infrasound record (Fig. 4b). The sound record also reveals a distinct slow phase at ~162 s (+24.4 s), i.e. ~ 3 min after the explosion. The available portion of the infrasound record is too short to see a corresponding signal. The ultrasound record shown in Fig. 4c is the longest (~ 4 min). The distinct phases in the ultrasound band around 40 s (+24.4 s), i.e. ~ 1 min after the explosion, may correspond to the lower-frequency arrivals around the same time in Fig. 4a and 4b. As high frequencies attenuate much faster than the lower frequencies, the arrivals in Fig. 4c appear more emergent than in Fig. 4a-b.

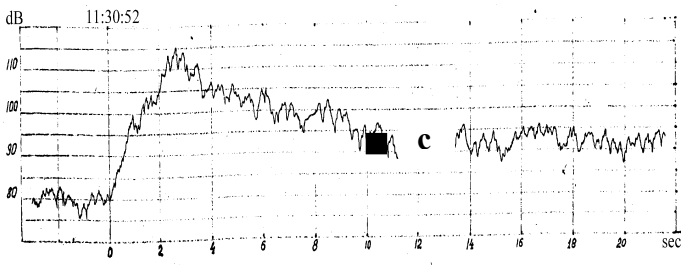


Figure 5 shows the available short portion of an infrasound record from the above-water 1961 nuclear explosion made at ~160-km distance. The pre-signal noise level is ~83 dB, while the signal level reaches ~115 dB. The 0 of the time axis is at 11:30:52 Moscow time, which is 25.4 s after explosion. The arrival seen at this time has traveled with an effective speed of ~6320 m/s, indicating likely reflection from the crust-mantle transition zone.

In an attempt to put these observations in perspective, we searched for relevant literature discussing coupling for shallow and above-water explosions. The *EM-I* (1996) manual lists relationships between pressure coupling coefficients and depth/height of blast, derived from theory of radiation hydrodynamics for low-yield non-radiative (<1 kt), high-yield radiative (>20 kt), and intermediate-yield (1 to 20 kt) nuclear sources. The coupling coefficient, ϵ , is given as a function of scaled charge depth, and is used to estimate the direct shock-wave peak pressure, $P_{\max} = A\epsilon/R^n$, where $A = f(n)$, $n = f(h)$, R is distance, and h is sensor depth; n approaches 1.13 for deep sensors (i.e., in free water), but is much larger for shallow sensors, in order to account for faster decrease of peak pressure with distance. Using a different approach, Clarke et al. (1995) at LLNL simulated the shock wave from a 1-kt nuclear explosion at 10 km, using a combination of a hydrodynamic code for the strong-shock calculations in the near field (distances <300 m) and a weak-shock calculation for the far field. Because of the very different set-up of the problem, comparisons with the *EM-I* relationships are likely inappropriate. One important difference is that in the LLNL calculations, full coupling is reached at a very large depth, $1000 \text{ m/kt}^{1/3}$, while in the *EM-I* relationships the coupling coefficients were set to 1 (i.e., to full coupling) at a very small charge depth, $4.5 \text{ m/kt}^{1/3}$. One might assume that these estimates (seemingly at two extremes) should be comparable at least for $0\text{-m/kt}^{1/3}$ charge depth (i.e., half-immersed charges). For such explosions, we calculated from the *EM-I* relationships $\epsilon = 0.2, 0.162, 0.11, \text{ and } 0.057$ for 1 kt, 5kt, 10 kt, and 16 kt, respectively. From the Clarke et al.'s pressure estimates, we calculated $\epsilon = 0.041$, which is close only to the 16-kt *EM-I* estimate, but is very different from the *EM-I* estimate for 1 kt. This illustrates the difficulty when attempting to bring together even results from two different modeling approaches, let alone observations and predictions.

For a 1.1-m charge height above water of the 16-kt 1961 explosion ($0.44\text{-m/kt}^{1/3}$ scaled height), we calculate $\epsilon = 0.0412$ from the *EM-I* relationships. Compared with 0.057 for a half-immersed charge, the difference is not large for this yield. Incidentally, the LLNL estimate, 0.041, is the same (only it is for a 1-kt yield). Thus the peak pressure of the direct shock wave from this explosion might be expected to be ~4 % of the pressure that would be measured from a deep charge. Using further the *EM-I* relationships, and converting the estimates in dB, we calculate that the free-water pressure levels from a 16-kt nuclear explosion are 158 dB at 35 km and 143 dB at 160 km. A 4 %-coefficient reduces these to 130 dB and 115 dB, respectively; the former is in excellent agreement with the level observed at 35 km in Fig. 4a, while the latter cannot be verified as the direct wave at 160 km arrives much later than the time window shown in Fig. 5.

The 4.8-kt 1961 underwater explosion at 20-m depth ($\sim 12\text{-m/kt}^{1/3}$ scaled depth) cannot be viewed in light of the *EM-I* coupling coefficients, because full coupling is assumed for such depths. Using the LLNL pressure estimates, we estimate that ϵ might be ~10%, interpolating between 0.041 for $0 \text{ m/kt}^{1/3}$ and 0.176 for $20 \text{ m/kt}^{1/3}$ (no pressure estimates available in between). This is a very crude estimate, especially because the LLNL calculations are only for 1 kt at 10 km. The free-water direct shock-wave pressure for this explosion are 154 dB at 35 km and 143 dB at 105 km. Thus the free-water estimate at 105 km for a 4.8-kt explosion is the same as the estimate for a 16-kt explosion at 160 km (see previous paragraph), which might have influenced the particular choices of yields and distances in the Russian tests. A ~10% coupling coefficient would reduce the pressure levels to 134 dB and 123 dB at the two distances. There is no observation in this time window at 105 km, but the observed level for the direct shock wave at 35 km is only ~100 dB in the infrasound record around ~24.4 s (Fig. 2b); this translates into an observed coupling coefficient of only 0.2%. Even lower level, < 70dB, is seen in the sound record at this time (Fig. 2a). As to the pressure level of ~103 dB observed for the arrivals reflected from the crust (~10-12 s at 35 km), it is the same as for the other 1961 explosion, given the difference in yields (4.8 kt vs. 16 kt) and positions in respect to the water surface (under and above); compare Fig. 2a (~12 s on the time axis) and 4a (~10 s on that time axis).

In addition to the arrivals of clearer origin discussed above, Figures 2 to 5 show phases likely due to multiple hydroacoustic reflections from the bottom, water surface and surrounding margins, known also as reverberations (*EM-I*, 1996). Due to much more efficient attenuation at higher frequencies, reverberations are relatively short-lived for frequencies exceeding 300 Hz. Shot Swordfish is cited in *EM-I* (1996) as the only nuclear explosion from which reverberation measurements were made at long ranges, but numerous

such measurements exist from HE explosions. Once in the water however, it does not matter in terms of reverberations if the energy originates from nuclear or HE sources.

In the 50's and 60's, the nuclear explosions in the Bay of Chernaya demonstrated the potential for a cover-up in shallow basins and reservoirs. Radioactive contamination stayed mostly in the bay and was not detected in the open sea. The acoustic waves from such explosions cannot reach the world sound channel at above-noise level and do not produce gas bubble phases as deep-water explosions do. The hydroacoustic energy is rather small by comparison with the energy transmitted in the air and the ground. Such explosions are thus not easily detectable with hydroacoustic means and could have posed a significant detection problem at that time. Today such nuclear blasts would be easily detected with the seismic network for CTBT monitoring. The closest U.S. analogues of these underwater explosions have been conducted in the West Pacific - Baker (1946, yield 23 kt, explosion depth 27 m, bottom depth 54 m) and Umbrella (1958, yield 8 kt, explosion on the bottom, bottom depth 45 m). All other U.S. underwater nuclear explosions have taken place in open-water, deep basins.

HE Explosions of 100-kg TNT in a Reservoir

Eneva et al. (1999) have reported earlier on some aspects of the 100-kg TNT reservoir explosions. These 1956 tests have been described and analyzed in several earlier Russian publications (e.g., Kozachenko and Khristoforov, 1970; Korobeinikov and Khristoforov, 1976). Twenty-nine 100-kg TNT experiments (charge radius ~ 0.25 m) were performed in a reservoir of length 87 m, depth 3 m, and width 25 to 55 m from bottom to top. Comprehensive measurements of shock wave time-histories and parameters (peak pressures, specific impulse and pulse duration) were made at various distances in water, air and ground. Most of the experiment configurations were applied twice, taking measurements at 7.5 m and 22.5 m from one of the explosions, and at 15 m and 30 m from the other. Sensor depths were varied from 0.25 m to 2.75 m, charge depths from 0 m (half-immersed) to 2.75 m, and water level from 3 m to 0.5 m. The bottom consisted of a layer of air-saturated sand, with a very low sound velocity (270 m/s), which for all practical purposes had an effect similar to the air above the water surface. These experiment configurations led to the observation of both regular and irregular reflections from the water surface and the bottom, depending on the locations of explosions and sensors. Eneva et al.'s work has been now extended to include analysis and modeling of additional shock wave parameters, such as positive pulse duration, and impulse and specific energy of the positive pulse. The latest 1999 REFMS version has been used to predict the measurements of shock-wave parameters.

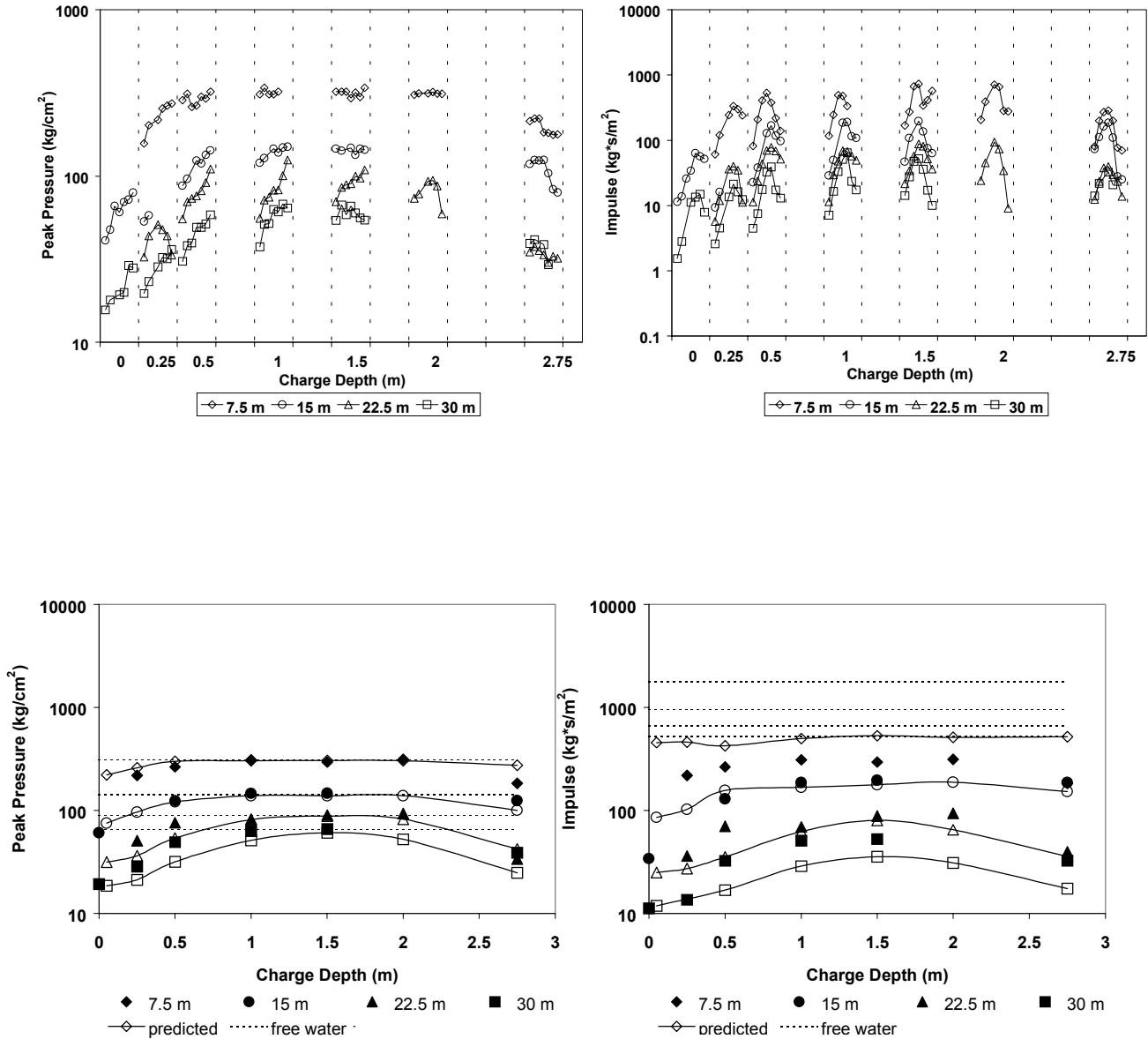
Impulse, pulse duration, and energy in boundless (free) water have been discussed in the classic work of Cole (1948). The pressure of the shock wave P (overpressure above the hydrostatic pressure), as a function of time t after arrival of the shock wave, is given by $P(t) = P_{\max} e^{-t/\theta}$, where P_{\max} is the initial peak pressure, and θ is so-called time constant, i.e., the time over which the pressure-time history can be approximated with an exponential decay. For many purposes, the effect of a shock wave depends on the time-integral of pressure, or impulse, more significantly than on the detailed form of pressure change with time. The specific impulse of unit area of the shock wavefront, up to a time τ after its arrival, is given by $I(\tau) = \int_0^{\tau} P(t) dt$. Another significant measure of the shock wave is energy flux density, E_f , representing the energy flux across unit area of a fixed surface normal to the direction of propagation (often referred to as energy flux, or simply energy); $E_f(\tau) \sim \int_0^{\tau} P^2(t) dt$. All these parameters can be represented by power laws $\sim 1/R^\alpha$, where R is distance from source and α is a constant. The empirical relationships given by Cole (1948) for HE charges of TNT, after modification of the units, are as follows:

$$(1) \quad P_{\max} = 533(W^{1/3}/R)^{1.13} \quad I = 588 W^{1/3}(W^{1/3}/R)^{0.89} \quad E_f = 8300 W^{1/3} (W^{1/3}/R)^{2.05},$$

where W is yield in kg (100-kg TNT in this case), and the impulse and energy flux are estimated in time $\tau = 6.6\theta$. The units in eq. (1) are m for distance, kg/cm^2 for pressure, $\text{kg}\cdot\text{s}/\text{m}^2$ for impulse, and $\text{kg}\cdot\text{m}/\text{m}^2$ for energy flux. These relationships show that the peak pressure decreases with distance faster than an

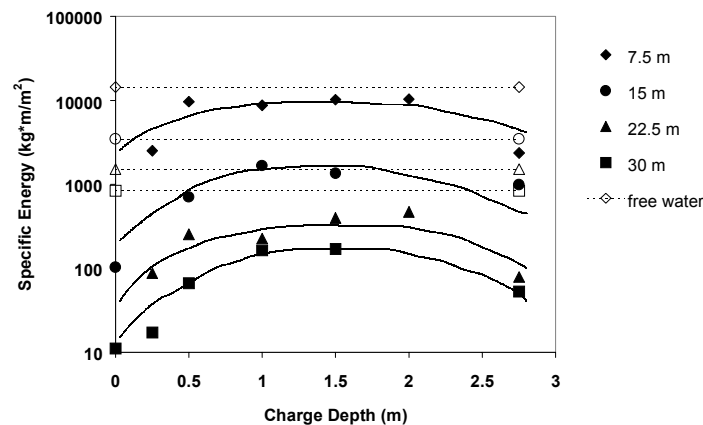
inversely proportional relationship (i.e., than acoustic approximation would imply), while the energy decreases faster than inversely proportional to the square root of the distance.

Figure 6 shows the peak-pressure and specific-impulse measurements from the twelve experiments, versus charge depth. The impulse is estimated over the duration τ_+ of the positive phase of the shock wave. The dependence of positive pulse duration, τ_+ , on explosion depth is similar to that of the impulse and is not shown. Data on measurement errors have not been found in the archives yet, but thirteen of the measurements at sensor depth 1.5 m have been taken by two different sensors for a given explosion and distance. The discrepancies between these are the smallest for the peak pressures (3.3% on average and not larger than 12.5%), larger for the pulse duration (9% on average, but as large as 33% in one case), and the largest for the impulse (14% on average, and as large as 28% in one case). The semi-symmetric appearance



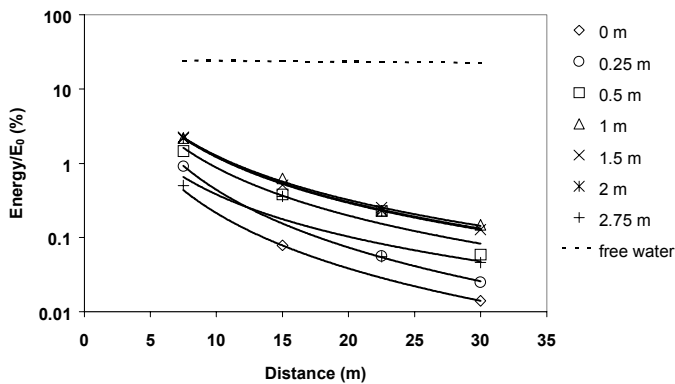
of the overall dependence of peak pressure on charge depth is due to the similar sound velocities of air and the sand on the bottom. Thus in the following we will mostly refer to results down to mid-pool depth. Fig. 6 shows a number of features of peak pressures: increase with charge depth, reaching maximum values around mid-pool; decrease with distance; mostly increase with sensor depth for any given shallow charge depth, but nearly constant values for mid-pool charge depths (especially closer to the explosions, at 7.5-m distance). The impulse also shows general increase with charge depth and decrease with distance. However, for any given explosion depth, the dependence on sensor depth is nearly symmetrical, with maximum reached around 1.5-m depth (mid-pool). This effect is due to reflections from the water surface and the bottom, which reduce the positive pulse duration, and therefore the impulse, when measurements are taken near the two boundaries. Kozachenko and Khristoforov (1970) have suggested semi-empirical formulae to fit the observations shown in Fig. 6, representing the shock-wave parameters through the free-water estimates in eq. (1) above, after application of certain correction factors. These correction factors are rather complicated functions of distance, sensor depth, and charge depths, and are not shown here.

Since measurements at 1.5-m depth are least affected by the boundaries, Figure 7 shows peak pressure and impulse measured at this depth, as a function of charge depth. Compared with peak-pressures from the REFMS modeling, the observed pressures indicate very good agreement in the near field (7.5 m and 15 m) and poorer fit further from the source. However, the fit is very good for charge depths around mid-pool at all distances. The impulse measurements agree with the REFMS predictions at mid-distances (15 m and 22.5 m), but appear rather overestimated closer to the source (7.5-m distance) and somewhat underestimated further from the source (30-m distance), except for small charge depths. These discrepancies may be related to additional reflections from the walls of the reservoir, not modeled at present. Fig. 7 also shows estimates in boundless water calculated from eq. (1). While observed and REFMS-predicted peak pressures fit these calculations very well for mid-reservoir charge depths, the impulse measurements are much lower. The reason for this is that pulse duration is undercut due to reflections from the boundaries, thus significantly reducing the impulse as compared with boundless water. As an example, note that the REFMS-predicted values at 7.5-m, already quite higher than the observations, are comparable with the free-water calculations at four times larger distances (30 m). These results show that in terms of peak pressures (but not impulse), explosions and measurements at depth of ~1.5-m approximate very well a free-water environment.

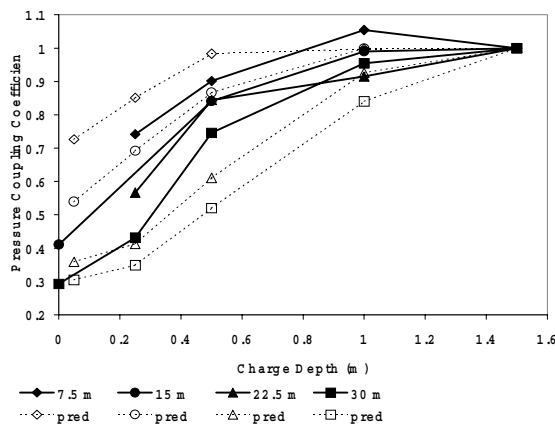


Similarly, specific energy of positive pulse, E_+ , measured at 1.5-m depth, is shown in Figure 8. These estimates are compared with calculations of the energy density flux in eq. (1), showing increasing departure for larger distances. Figure 9 shows the dependence of shock-wave energy, as a portion of total energy of explosion ($418 \times 10^3 \text{ kg}\cdot\text{m} = 418 \text{ MJ}$ for 100-kg TNT), on distance to sensor. The shock-wave energy in this case is calculated as $2\pi R \int_0^H E_+(h) dh$, where h is sensor depth, $E_+(0) = 0$ and H is the maximum sensor depth (2.75 m in these experiments). At 23-24%, the free-water estimates in Fig. 9 are much higher than the observed values, which exceed 1 to 2% only in the near field, and are measured at hundreds of a per cent further from the source. A distinct dependence on charge depth is indicated; for any given distance, these estimates are generally lowest for half-immersed charges (0-m depth), higher for 0.25-m and 2.75-m depths closer to the boundaries, still higher for 0.5-m depth, and the highest for mid-pool charge depths (1 m, 1.5 m, and 2 m).

Finally, Figure 10 shows what could be considered as a coupling coefficient in terms of pressure, versus



charge depth. This coefficient is estimated by dividing the peak pressures from various charge depths by the pressure from a mid-pool explosion, best approximating a boundless-water environment. All measurements are taken at mid-pool, i.e., at 1.5-m depth. It is evident that these coefficients decrease as the charge approaches the surface, and the rate of this decrease is faster for larger distances. The character of the REFMS-predicted changes is the same, but a good match between observations and predictions is only seen at 15-m distance, i.e., neither too close nor too far from the source. In general, the REFMS modeling overestimates the observations in the near field (7.5 m and 15 m), possibly because in the real reservoir more energy is lost to reflections in the



reservoir walls. Conversely, further from the source (22.5 and 30 m), peak pressures tend to decrease with charge depth more slowly than predicted, except perhaps on the surface (half-immersed charges).

In addition to the relationships for pressure coupling coefficients from nuclear explosions, *EM-1* (1996) also lists a simpler relationship for HE explosions of all sizes. These coefficients are much higher and change much more slowly with charge depth, than those for nuclear blasts. The small charge depth of $4.5 \text{ m/kt}^{1/3}$, for which full coupling is assumed in the *EM-1* manual, translates into less than 0.25 m in the 100-kg TNT case, using a scaling

factor of $0.046416 = (0.0001 \text{ kt})^{1/3}$. Thus, only the observations from a half-immersed charge (0-m depth), $\epsilon = 0.41$ at 15 m and $\epsilon = 0.29$ at 30 m, can be compared with the analogous *EM-I* HE estimate of $\epsilon = 0.89$ at $0 \text{ m/kt}^{1/3}$. Thus, our data not only show significantly smaller estimates for ϵ , but also reveal a dependence on distance that is absent in the *EM-I* relationships.

CONCLUSIONS AND RECOMMENDATIONS

Unique historic Russian data sets from three nuclear explosions in the shallow waters of the Bay of Chernaya (Novaya Zemlya) and 100-kg TNT reservoir explosions have been examined and analyzed for the purpose of characterizing the effect of charge depth on the hydroacoustic signals. This is of interest to CTBT monitoring because of the diminished signal levels from shallow explosions as compared to fully immersed charges. We have made various estimates to compare with existing relationships describing the coupling of hydroacoustic energy. We have also modeled the small-scale HE explosions, using the REFMS code for modeling of shock waves in water. The hydrophone records from the nuclear explosions recorded near and further from the source, shed light on the type of arrivals and pressure levels observed from such explosions. In particular, the pressure level of direct shock wave from the 1961 above-water blast appears diminished to about 4% of the free-water pressure at 35 km, in agreement with existing coupling relationships. The pressure levels from the underwater nuclear explosions are less well understood in this respect. The 100-kg TNT experiments and the REFMS-predicted peak pressures indicate coupling coefficients in the range of 30 to 70 % for half-immersed charges, depending on distance, gradually increasing to full coupling in mid-pool, where the conditions can be approximated with free-water regime.

These observations and results suggest that the effect of charge depth on the hydroacoustic shock-wave energy is more complicated than currently accounted for by existing relationships. Thus these relationships may have to be adjusted, while the relevance of the effect of charge depth in small-scale HE shallow experiments to the effect of depth of nuclear explosions needs further investigation.

ACKNOWLEDGEMENTS

We thank Bob Britt (SAIC) and Bob Thrun (NSWC) for providing the latest version of the REFMS code. Bob Britt was also very helpful with explanations of this software. Norton Rimer (Maxwell) is thanked for discussions and Chuck Wilson (Maxwell) has continued to advise us on the relevant literature.

REFERENCES

- Eneva, M., J.L. Stevens, J. Murphy, B.D. Khristoforov, and V.V. Adushkin, Analysis of Russian hydroacoustic data for CTBT verification, in *Proc. 21st Seis. Res. Symp., 21-24 Sep., 1999*, Dept. Defense LA-UR-99-4700, 25-35, 1999. (Also accepted for publication in *Pure Appl. Geophys.*, 2001).
- Britt, J.R., *Shock Wave Reflection and Refraction in Multi-Layered Ocean/Ocean Bottom – A User's Manual for the REFM Code*, SAIC, DNA TR-86-49, January 1986 (U).
- Clarke, D.B., J.W. White, and D.B. Harris, *Hydroacoustic Coupling Calculations for Underwater and Near-Surface Explosions*, Lawrence Livermore National Laboratory, UCRL-ID-122098, 1995.
- Cole, R.H., *Underwater Explosions*, Princeton University Press, Princeton, New Jersey, 1948.
- Handbook of Nuclear Weapon Effects: Calculational Tools Abstracted from DSWA's Effects Manual One (EM-I)*, ed. J. Northrop, DSWA, pp. 736, 1996 (U).
- Korobeinikov, V.P. and B.D. Khristoforov, Underwater explosions: Summary of Science and Technology, *Hydromechanics* **9**, 54-119, 1976 [in Russian].
- Kozachenko, L.S. and B.D. Khristoforov, Shock waves in a shallow-water reservoir, *J. Appl. Mech. Tech. Phys.* **4**, 166-171, 1970 [in Russian].
- Stephens, T. and C.S. Kelly, Computational Aids Update, *Science & Technology Digest*, August, 42-43, 1996.
- USSR Nuclear Weapons Tests and Peaceful Nuclear Explosions 1949 through 1990*, Ministry of the Russian Federation for Atomic Energy, ISBN 5-85165-062-1, pp. 63, 1996.